The 2009 IEEE/RSJ International Conference on
Intelligent Robots and Systems
October 11-15, 2009 St. Louis, USA

Experimental verification of antagonistic stiffness planning for a 2-DOF planar parallel manipulator

Sungcheul Lee, Woosung In, Sitai Kim, Jay I. Jeong and Jongwon Kim

Abstract— **In this paper, two torque assignment methods of the antagonistic stiffness for a 2-DOF planar parallel manipulator are presented and verified by experiments. The first method is equalizing the magnitude of the stiffness in all directions at a desired position. The second method is maximizing the active stiffness in one direction at a given path. A 2-DOF parallel mechanism with four actuators is used for verification tests, where the internal torque of the mechanism exists on the two dimensional null space. In the experiment, passive and active stiffness are tested when endowing the external force at the moving platform and compared with the estimated results.**

I. Introduction

THE stiffness of a manipulator is categorized into passive stiffness and active (antagonistic) stiffness. Passive stiffness is related to joint stiffness and kinematic constraints, which depend on the position of the end-effector. For a redundantly actuated parallel mechanism that has excessive actuators to the degrees of freedom, a resistive action to external forces can be generated by controlling the internal torques on additional motors. This action is called as antagonism in static equilibrium.

As previous works for the stiffness of the parallel mechanism, Gosselin[1] developed passive stiffness maps for the workspace of several manipulators. Kim et al.[2], Ceccarelli and Carbone[3] and Li and Xu[4] also presented stiffness analysis for several kinematic mechanisms[5-8]. Regarding the active stiffness, stiffness control methods are also showed[9-12]. Kock and Schumacher[13] presented a control scheme which guarantees the lower bound of an end-effector stiffness. Müller[14] showed that the internal force can be used to eliminate the backlash of parallel mechanisms. Chakarov[15] showed that maximum compliance in certain directions can be reduced by controlling the distribution of linear motor torques. He focused on finding eigenvalues of the compliance matrix. Kim et al.[16] did kinematic analysis of 2-DOF manipulator and validated that the internal preload can increase the stiffness by experiment.

In this paper, we present two assignment methods of the antagonistic stiffness planning for a two degrees-of-freedom planar parallel manipulator and verify them by experiments. We design two indices for the stiffness planning. The first index that is the ratio of maximum stiffness to minimum stiffness at a given point represents the distribution of the active (antagonistic) stiffness at a given point when external forces with random direction are applied to the mechanism. The index is designed to ensure robustness of antagonistic stiffness in all directions.

The second index represents the maximum stiffness value for an external force with fixed direction. The index can be used to increase the stiffness of the mechanisms in one direction when an external force with constant direction is applied to the end-effector. When a directional disturbance such as gravity is applied to the mechanism, the control strategy that maximizes the stiffness of the mechanism in that direction will be helpful to compensate the constant external force.

This paper is organized as follows. In section 2, the theoretical formulation and simulation of the stiffness analysis are described. The two indices are introduced and stiffness estimations are presented in section 3. In section 4, the indices are validated by the experiment and the results are presented. Finally, the conclusion follows in section 5.

II. Stiffness Analysis and Simulation

Generally, the stiffness is defined as the ratio between the exerted force and the displacement of the end-effector. Therefore, the stiffness matrix K is related with the change of the external force Δf and the displacement of the platform Δx_c. The relationship is described in (1)

$$K = \lim_{\Delta x_c \to 0} \frac{\Delta f}{\Delta x_c} = \frac{df}{dx_c} \tag{1}$$

where, $K = \begin{bmatrix} K_{xx} & K_{xy} \\ K_{yx} & K_{yy} \end{bmatrix}$, $\Delta f = \begin{bmatrix} \Delta f_x \\ \Delta f_y \end{bmatrix}$, $\Delta x_c = \begin{bmatrix} \Delta x_x \\ \Delta x_y \end{bmatrix}$.

Manuscript received March 1, 2009. This paper was supported by the second stage of the Brain Korea 21 Project for Seoul National University, by the Seoul R&BD Program (Grant No. 10583), and by the research program 2008 of Kookmin University in Korea.

Sungcheul Lee and Woosung In are with School of Mechanical and Aerospace Engineering, Seoul National University, Sillim 9-Dong, Gwanak-Gu, Seoul, South Korea, 151-744 (e-mail: sclee@snu.ac.kr wsin@rodel.snu.ac.kr).

Sitai Kim is with Department of Mechanical Engineering, Korea Air Force Academy, P.O. Box, 335-1, Ssangsu-Ri, Namil-Myeon, Cheongwon-Gun, Chungbuk, South, Korea 363-849 (e-mail: sitaikim@gmail.com).

Jay I. Jeong is with of Mechanical and Automotive Engineering, Kookmin University, 861-1 Jeongneung-Dong, Songbuk-Gu, Seoul, South Korea, 136-702 (corresponding author; phone: +82-2-910-4419; fax: +82-2-910-4839; e-mail: jayjeong@kookmin.ac.kr).

Jongwon Kim is with School of Mechanical and Aerospace Engineering, Seoul National University, Sillim 9-Dong, Gwanak-Gu, Seoul, South Korea, 151-744 (e-mail: jongkim@snu.ac.kr).

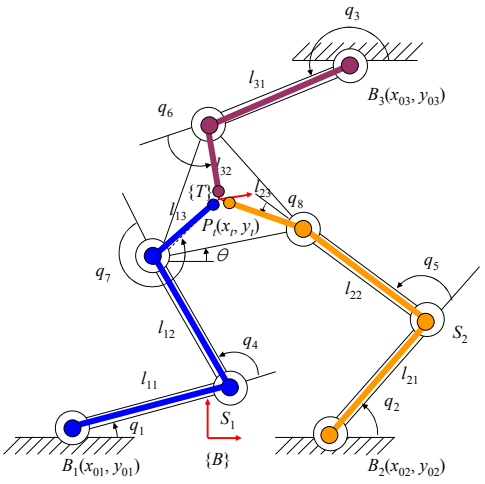

Fig. 1. Schematic of a 2-DOF parallel mechanism

The Δf_x and the Δf_y are the X and Y directional forces, respectively. The Δx_x is the X directional displacement and the Δx_y is the Y directional one.

The stiffness matrix K can be derived as below:

$$K = \frac{df}{dx_c} = \frac{d\Psi^T \tau_r}{dx_c} = H^T \tau_r + \Psi^T \frac{d\tau_r}{dx_c} = H^T \tau_r + \Psi^T \frac{d\tau_r}{dq_r} \Psi \tag{2}$$

$$K = H^T \tau_r + \Psi^T K_r \Psi = K_{active} + K_{passive}, \tag{3}$$

where $\Psi \equiv \frac{dq_r}{dx_c}$, and $\frac{d\tau_r}{dx_c} = \frac{d\tau_r}{dq_r}\frac{dq_r}{dx_c} = \frac{d\tau_r}{dq_r}\Psi$

The $\partial \tau_r / \partial q_r$, is defined as the diagonal matrix, $K_r = diag(k_1, k_2, k_3, k_4)$ and k_i is the torsional stiffness of the i-th actuating joint.

The passive stiffness, $K_{passive}$, of a manipulator is related with the configuration of the mechanism and the torsional stiffness of the actuating joints k_i in the static state. When r numbers of active actuators are assembled at the 2-DOF planar manipulator, the passive stiffness can be written as (4).

$$K_{passive} = \Psi^T K_r \Psi = \begin{bmatrix} k_{xx} & k_{xy} \\ k_{yx} & k_{yy} \end{bmatrix}. \tag{4}$$

The active stiffness, K_{active}, of a redundant parallel manipulator is a function of the internal torque at the equilibrium state. At the internal equilibrium state the active stiffness can be written as (5)

$$K_{active} = H^T \tau_r \tag{5}$$

where $H = \frac{\partial \Psi}{\partial x_c} = \frac{\partial \Psi}{\partial q_r}\frac{\partial q_r}{\partial x_c} = \frac{\partial (\Gamma J_f^{-1})}{\partial q_r}\Psi = \left(\frac{\partial \Gamma}{\partial q_r} J_f^{-1} + \Gamma \frac{\partial J_f^{-1}}{\partial q_r}\right)\Psi$.

The internal torque can be calculated by inverse dynamic analysis of the mechanism given. If the mechanism is a non-redundant actuated manipulator, the solution of the inverse dynamics is unique and can be obtained from the dynamic modeling and the constraint of the mechanism. However, a redundant actuated manipulator can give indeterminate solution at the same motion state.

We defined the torque applied to the independent joint as τ_u and the torque of the active joint as τ_r, and then determined the relationship between these torques. By the virtual work theorem, the relationship between the two kinds of torque can be shown as follows

$$\tau_u^T \dot{q}_u = \tau_r^T \dot{q}_r, \tag{6}$$

$$\tau_u^T \dot{q}_u = \tau_r^T (\Gamma \dot{q}_u), \tag{7}$$

$$\tau_u = \Gamma^T \tau_r \tag{8}$$

$$\tau_r = \left(\Gamma^T\right)^+ \tau_u + \left(I_r - \left(\Gamma^T\right)^+ \Gamma^T\right)\varepsilon_r = \tau_{r,motion} + \tau_{r,internal} \tag{9}$$

where $\dot{q}_r = \partial f / \partial q_u \, \dot{q}_u = \Gamma \dot{q}_u$. The operator, $(\cdot)^+$, is defined as the generalized inverse or pseudo inverse. The ε_r is an arbitrary vector that determines the magnitude of the internal torque. The independent joint torque τ_u is zero in the case of the static state. The relationship of internal torques among the active joints can be calculated as follows

$$\Gamma^T \left(I_r - \left(\Gamma^T\right)^+ \Gamma^T\right)\varepsilon_r = \begin{bmatrix} 0 \\ 0 \end{bmatrix} = \Gamma^T \tau_r. \tag{10}$$

We conduct a simulation to calculate the active stiffness at the point of (-100mm, 250mm). The simulation condition is presented in TABLE I and Fig. 2. An external force was assumed to be induced at the center of the platform and then the displacement by the force was calculated. We repeated the same procedure with the various forces that direction were assigned from 0° to 360° in 5° step. The displacement of the platform by each external force is depicted as a circular mark in Fig. 3. The position of each mark adopts the direction of the induced force and the magnitude of the displacement from the origin.

The maximum torque capacity of the actuators should be considered to manipulate the active stiffness of the mechanism. Moreover, the actuating torque τ_{r1} and τ_{r2} are function of τ_{r3} and τ_{r4} in the internal torque equilibrium state. In Fig. 3(a), the maximum capacity limits of τ_{r1} and τ_{r2} are presented in the stiffness map of τ_{r3} and τ_{r4}, where limits of τ_{r1} and τ_{r2} is depicted as a white color at top right side and bottom left side.

In Fig. 3(b)-3(d), the distribution of compliance are presented with respect to the internal torque τ_{r3} and τ_{r4}. In the figures, the compliance shape resembles a figure of a snowman. The result shows that the magnitude and the shape of compliance are controllable. Fig. 3(b) presents the passive compliance when there is no internal force in the mechanism.

In Fig. 3(c), the compliance is shown when 0Nm and 10.4Nm are imposed as the internal torque τ_{r3} and τ_{r4}. In the figure,

TABLE I
SIMULATION PARAMETERS FOR ACTIVE STIFFNESS ENHANCEMENT

Quantity	Values
Torsional stiffness, k_r	10Nm/rad
Maximum internal torque($\tau_{r,max}$)	10.5Nm
Platform position, P_t	(-100mm, 250mm)
External force	2.5N
Step of degree	5°
Link lengths (l_{11} , l_{12} , l_{21} , l_{22} , l_{31})	280mm
Length of a side of platform, t	210mm
Base revolute joint coordinate, B_i	B_1(-300,0), B_2(300,0), B_3(150, 420)

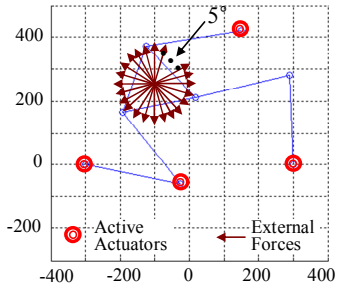

Fig. 2. Kinematic configuration of the 2-DOF mechanism at the position (-100, 250)

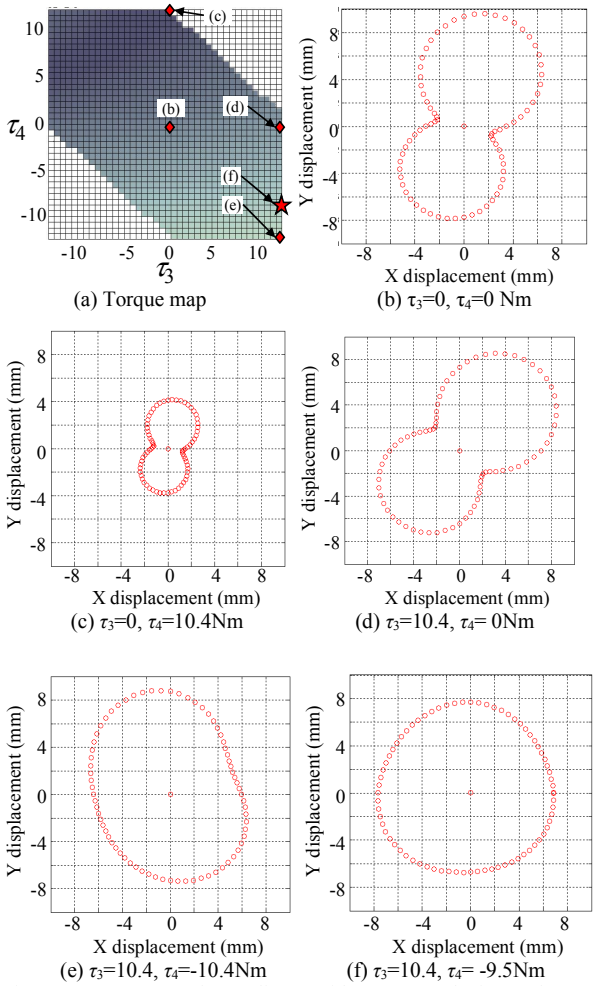

Fig. 3. Torque map and compliance with respect to the internal torque assignment caption.

the average magnitude of the compliance changed compared with the passive compliance case. However, the shape of the compliance is observed to be similar to Fig. 3(b). In contrast, in Fig. 3(d), the shape of the compliance is changed when the internal torque τ_{r3} and τ_{r4} are set as 10.4Nm and 0Nm, respectively. The Fig. 3(e) and Fig. 3(f) show that the overall shape of the compliance is changed. These results reflect the possibility of stiffness planning by changing the internal torque distribution.

III. STIFFNESS PLANNING

The stiffness planning for a redundantly actuated manipulator is to determine the torque distribution of the actuating joint to make the designed end-effector stiffness. Here, we used the compliance to represent the relationship between the distributed torques and the displacements of the end-effector. The inverse of the stiffness matrix is defined as the compliance matrix and it also shows the relationship of the force and displacement.

$$\Delta f = S(\tau)\Delta x_c \tag{11}$$

$$\Delta x_c = C(\tau)\Delta f \tag{12}$$

where the Δf is the external force. The Δx_c is the displacement vector by the force. The compliance, $C(\tau)$, that is the inverse of the stiffness, $S(\tau)$, is defined as the displacement divided by the given directional force as follows

$$C(\tau) = \frac{1}{S(\tau)} = \frac{\|\Delta x_c\|}{\|\Delta f\|} \quad . \tag{13}$$

A. *Equalize the Stiffness in all stiffness (I_R)*

In some cases, the displacement of the end-effector due to the external force should remain within predefined presets even though any force in random direction is applied to the mechanism. Thus, a method for optimizing the internal torque distribution is required in order to minimize the displacement due to any directional forces.

The goal of the stiffness planning is related to the robustness and balance of the stiffness of the manipulator when the external force is given randomly. We define an index I_R, as the ratio of the minimum to maximum stiffness as follows:

$$I_R = \frac{\min\left(\|\Delta x\|_d\right)}{\max\left(\|\Delta x\|_d\right)}, \; d = 0,\ldots,360°, \tag{14}$$

where d is the index of the force direction, which covers 360 degrees. The Δx is directional displacement when the directional forces Δf_d are imposed.

By maximizing the index I_R, the ratio between the minimum value and the maximum value should approach the unity value. The displacement due to the external force will be balanced by determining the optimal distribution of

internal torques. We can express the strategy for maximizing the index I_R as follows:

$$\max_{\tau_r}\left(I_R\right) \text{ when } \quad \left|\tau_r\right| \le \tau_{r,\max} \tag{15}$$

where the τ_r is the internal torque vector that includes all torques in the actuating joints of the platform. The $\tau_{r,\max}$ is the maximum torque limit of the actuators installed.

B. *Maximize the stiffness in one direction* (I_D)

The high stiffness in the predefined direction is often required in some cases such as cutting or drilling processes for reducing the positional error. We define the index that can reflect the maximum stiffness when a directional disturbance is continuously imposed at the center of the platform. Mathematically, the index can be expressed as the ratio of the change of the external force to that of the displacement norm as follows:

$$I_D = \frac{\left\|\Delta f_c\right\|}{\left\|\Delta x_c\right\|} \tag{16}$$

where Δf_c is a external disturbance with a fixed direction. The Δx_c is the directional displacement when the external force Δf_c is imposed at the center of the platform.

The strategy for enforcing a predefined directional stiffness can be written as

$$\max_{\tau_r}\left(I_D\right) \text{ when } \quad \left|\tau_r\right| \le \tau_{r,\max} . \tag{17}$$

C. *Installation position of actuators*

Since there are two excessive actuators to the mobility of the mechanism in this study, we have to determine the installation position of the actuators. One strategy for selecting the actuator position is maximizing the index I_R in the workspace of the given mechanism. By maximizing I_R in the workspace, we can use maximum internal torque to enhance the active stiffness.

For the mechanism in this study, the four actuators can be installed at the eight joints that include three base joints. Because of the easiness of the installation, three actuators are attached at the base joints. So, one additional actuator should be located among the other five joints. The simulation parameters are presented in TABLE II and Fig. 4.

We selected the four points that represent the workspace to test the index I_R and the average of the index values at the test points are calculated. The result of the estimation is shown in TABLE III. The average of the ratio of the minimum to maximum stiffness is the largest when the actuator is attached at joint #6.

IV. Experimental Verification

This section presents the experimental verification of the stiffness analysis. First of all, we measured the torsional stiffness of each joint to calculate the passive stiffness of the mechanism. Then, we conducted the experiment to measure the passive stiffness. The active stiffness by endowing the internal torque also tested and measured. The difference between the calculated data and the experimental data is

TABLE II
SIMULATION PARAMETERS FOR DETERMINING INSTALLATION POSITION OF ACTUATORS

Quantity	Values
Torsional stiffness, k_1, k_2, k_3, k_4	13.2, 12.1, 19.9, 15.4 Nm/rad
Maximum internal torque ($\tau_{r,\max}$)	8.7 Nm
Platform position, P_t (mm, mm)	P_{t1}(50, 150), P_{t2}(0, 200), P_{t3}(-100, 250), P_{t4}(-150, 400)
External force	7.8 N
Step of degree	5º
Link lengths (l_{11}, l_{12}, l_{21}, l_{22}, l_{31})	280 mm
Length of a side of platform, t	210 mm
Base revolute joint coordinate, B_i	B_1(-300,0), B_2(300,0), B_3(150, 420)

TABLE III
RESULT OF INSTALLATION POSITION OF ACTUATORS

Joint	THE RATIO OF MIN. TO MAX. STIFFNESS (INDEX #1)				
	P_{t1} (50, 150)	P_{t2} (0, 200)	P_{t3} (-100, 250)	P_{t4} (-150, 400)	Avg.
4	0.1999	0.7702	0.3740	0.2260	0.3925
5	0.6708	0.9405	0.3904	0.1869	0.5472
6	0.7001	0.9148	0.5043	0.2381	0.5893
7	0.1639	0.1350	0.1055	0.1936	0.1495
8	0.1778	0.1960	0.3360	0.4348	0.2861

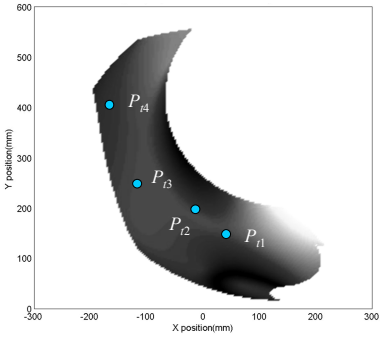

Fig. 4. Selected positions for estimated #1assignment caption.

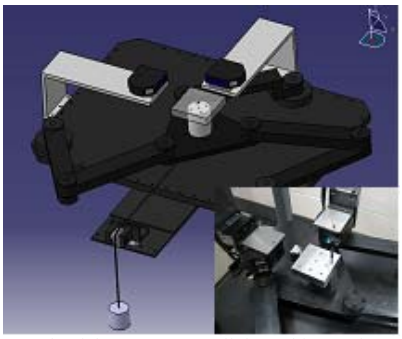

Fig. 5. Photograph of the 2-DOF parallel machine and controller.

TABLE IV
THE SPECIFICATION OF LASER SENSORS

Keyence Sensor	LB-11	LK-031
Accuracy	0.01 mm	0.001 mm

examined. The experimental system is depicted in Fig. 5.

In order to calculate the passive and active stiffness of the mechanism, the torsional stiffness of the actuating joints and the torque distribution should be known.

To measure the stiffness of each joint, at first, a weight of 50 gram is imposed as the preload to eliminate the effect of the backlash, and then the displacement of the end of each link is measured by adding 50 gram weights one by one. After this process is repeated three times, the same method is used for the opposite direction. The average stiffness of each joint is shown in TABLE V.

TABLE V
INPUT PARAMETERS AT (0, 200).

Quantity	Values
Platform position, P_t	(0, 200)
Torsional stiffness, k_r	13.2, 12.1, 19.9, 15.4 Nm/rad
Internal Torque, τ_r	-6.9, 7.7, 3.1, 5.1 Nm
Maximum internal torque, $\tau_{r,max}$	8.7 Nm
External force	7.8 N + 0.5 N , 30º Step

A. Experiment of equalizing the stiffness in all directions (Exp. #1)

In this section, the antagonistic stiffness planning experiment is conducted at specific positions within the workspace when the actuator is located at the joint #1, #2, #3, and #6. The optimal index I_R that is defined in section 3, is used to execute the stiffness planning.

We executed the experiment for the active stiffness using I_R at one position, $P_{t2}(0, 200)$. The directional forces are endowed from 0° to 360° by 30° step. After this process is repeated three times, the average of these data is recorded for the stiffness value. The experimental condition is presented in TABLE V and Fig. 6. With the optimal distribution of internal torque at $P_{t2}(0, 200)$, the result of the experiments is depicted in Fig. 7 and Fig. 8. The experimental values of index I_R were obtained as 0.32 for the passive stiffness case and 0.64 for the optimized active stiffness. The calculated index value of I_R was 0.22 as the passive case and 0.93 as the active case, respectively. The difference between the estimated result and the experimental result is 12.3% at the passive case, and 10.7% at the active case.

The difference between the simulation and the experimental results is inferred from the linearization error in calculation of the displacement by using Jacobian. When the displacement by the external force is relative large, the assumption that the displacement is supposed to be small and the displacement of the end-effector can not be calculated from linear assumption of the Jacobian analysis. The friction that exists on the internal parts of the mechanism is supposed to be another cause of the difference since the hysteresis can be induced by the friction.

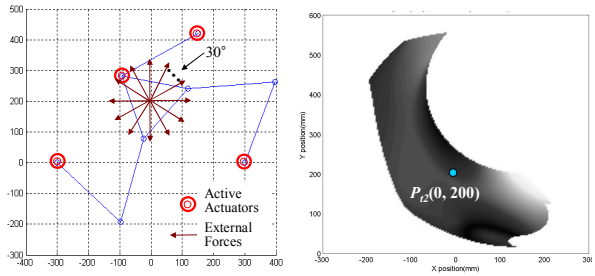

Fig. 6. Schematic diagram and position at (0, 200)

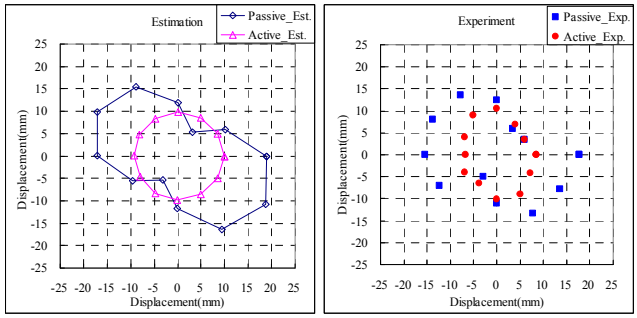

Fig. 7. Estimated vs. Tested result at (0, 200)

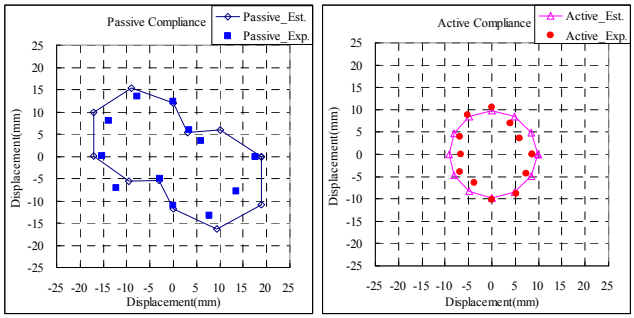

Fig. 8. Passive vs. active compliance result at (0, 200)

B. Experiment of maximizing the stiffness in one direction (Exp. #2)

The optimal index I_D that is defined in section 3 was used to accomplish the stiffness planning against a fixed directional force. The active stiffness is designed to be maximized in one direction by maximizing the index I_D.

The experiment was conducted along the representative pathway through the origin. The end-effector position of 11 points from (100, 200)mm to (-100, 200)mm by 20 mm were selected for the stiffness optimization. The preload same as previous experiment is given to eliminate the backlash of the mechanism. The end-effector was moving along the –X direction while external force was endowed along the –Y direction. After this process was repeated three times, the average of the displacement was recorded as the compliance value. The experimental parameters are described in TABLE VI and Fig. 9.

The experimental results are depicted in Fig. 10 and Fig. 11. While the estimated value of index I_D increased from 0.85 N/mm in the passive case to 1.03 N/mm in the active case, the experimental value of index I_D increased from 0.83 (passive) to 1.09 (active). While the estimated increment ratio is 22.8%, the experimental increment ratio is 32.2%. This says that we can get better results in the experiment than in the estimation. The difference between the calculation and the experimental result is estimated as 2.9% at the passive case, and 5.7% at the active case. These are very similar values.

TABLE VI
EXPERIMENTAL PARAMETERS FOR EXPERIMENT #2

Quantity	Values
Platform position, P_t	From (100, 200) to (-100, 200), Step -20
Torsional stiffness, k_r	13.2, 12.1, 19.9, 15.4 Nm/rad
Maximum internal torque, $\tau_{r,max}$	8.7 Nm
External force	7.8 N + 0.5 N , -Y direction

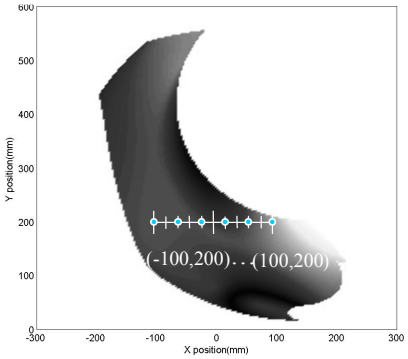

Fig. 9. The selected positions within the workspace

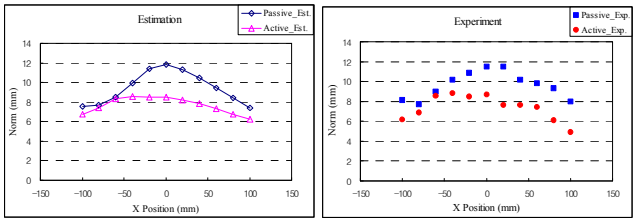

Fig. 10. Estimated and experimental result at the given path

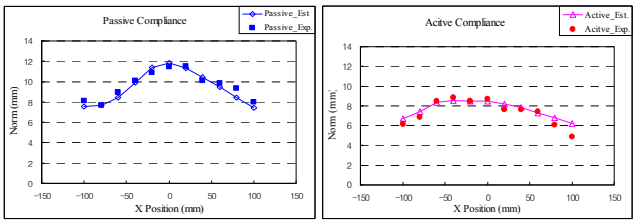

Fig. 11. Passive and active compliance result at the given path

In Fig. 10, the displacement of the passive stiffness and that of the active stiffness seem to be similar at point (-60, 200) or (-80, 200), since the maximum active stiffness is restricted by torque capacity of the actuators.

V. CONCLUSION

In this paper, we carried out a theoretical evaluation of the antagonistic stiffness analysis and applied it to a 2-DOF planar parallel manipulator. The Jacobian, the Hessian and the stiffness analysis were investigated. Two methods for the active stiffness planning were presented. The index I_R was suggested to make the minimum stiffness similar to the maximum stiffness at a given point and to ensure robustness and balance of the stiffness in all directions. Another index I_D was used to maximize the stiffness in a fixed direction along the pathway. The simulation and experiment are executed about a 2-DOF parallel mechanism to maximize the two indices. The experimental index I_R was observed to increase by 100% from 0.32 (passive) to 0.64 (active) at (0, 200). The average experimental index I_D was observed to increase by 32.2% from 0.83 (passive) to 1.09 (active) along the representative pathway.

REFERENCES

[1] C. Gosselin and J. Angeles, "Singularity Analysis of Closed-Loop Kinematic Chains," IEEE Transactions on Robotics and Automation, Vol. 6, 1990, pp. 281-290.

[2] J. Kim, F.C. Park, S.J. Ryu, J. Kim, J.C. Hwang, C. Park, C.C. Iurascu, "Design and Analysis of a Redundantly Actuated Parallel Mechanism for Rapid Machining," IEEE Transaction on Robotics & Automation, Vol. 17, No. 4, 2001, pp. 423-434.

[3] M. Ceccarelli, G. Carbone, "A Stiffness Analysis for CaPaMan(Cassino Parallel Manipulator)," Mechanism and Machine Theory, Vol. 37, 2002, pp. 427-439.

[4] Y. Li, Q. Xu, "Kinematics and Stiffness Analysis for a General 3-PRS Spatial Parallel Mechanism," *Proceeding of 15th CISM-IF to MM Symposium on Robot Design, Dynamics and Control, Montreal, Canada Romansy*, 2004.

[5] G. Carbone, M. Ceccarelli, "Experimental Tests on Feasible Operation of a Finger Mechanism in the LARM Hand," International Journal Mechanics Based Design of Structures and Machines, vol.36, 2008, pp.1-13.

[6] G. Carbone, "Stiffness Performance of Multibody Robotic Systems" *IEEE-TTTC International Conference on Automation, Quality&Testing, Robotics AQTR 2006*, vol.2, 2006, pp.219-224.

[7] G. Carbone G., M. Ceccarelli,"A Comparison of Indices for Stiffness Performance Evaluation," *12th World Congress in Mechanism and Machine Science IFToMM, Besançon*, paper n.A831, 2007.

[8] Huang S., Schimmels J.M.,"Achieving an Arbitrary Spatial Stiffness with Springs Connected in Parallel," ASME Journal of Mechanical Design, vol.120, n.4, 1998, pp.520-526.

[9] B.J. Yi, R.A. Freeman, D. Tesar, "Open-loop Stiffness Control of Overconstrained Mechanisms/Robotic Linkage Systems," *Proceedings of the IEEE International Conference on Robotics & Automation*, Scottsdale, Vol. 3, 1989, pp. 1340-1345.

[10] En English C.E., Russell D.,"Mechanics and Stiffness Limitations of a Variable Stiffness Actuator for Use in Prosthetic Limbs," Mechanism and Machine Theory, vol.34, n.1,1999, pp.7-25.

[11] Shane A. Migliore, Edgar A. Brown, and Stephen P. DeWeerth, "Biologically Inspired Joint Stiffness Control," *Proceedings of the 2005 IEEE International Conference on Robotics and Automation Barcelona, Spain,* April 2005, pp.4508-4513

[12] W.L. Chan, D. Arbelaez, F. bossens, and R.E. Skelton."Active vibration control of a three-stage tensegrity structure," *SPIE 11th Annual International Symposium on Smart Structures and Materials*, San Diego, March 2004.

[13] S. Kock, W. Schumacher, "A Parallel X-Y Manipulator with Actuation Redundancy for High-Speed and Active-Stiffness Applications," *Proceedings of the IEEE International Conference on Robotics & Automation*, Leuven, 1998, pp. 2295-2300.

[14] A. Müller, "Internal Preload Control of Redundantly Actuated Parallel Manipulator - Its Application to Backlash Avoiding Control," IEEE Transactions on Robotics & Automation, Vol. 21, 2005, pp. 668-677.

[15] D. Chakarov, "Study of the antagonistic stiffness of parallel manipulators with actuation redundancy," Mechanism and Machine Theory, Vol. 39, 2004, pp. 583-601.

[16] S. Kim, W. In, H. Yim, J.I. Jeong, F.C. Park and J. Kim, "Stiffness enhancement of a redundantly actuated parallel manipulator using internal preload: Application to a 2-d.o.f parallel mechanism," *Asian Symposium for Precision Engineering and Nanotechnology*, 2007.